Cell transfection *in vitro* and *in vivo* with nontoxic TAT peptide-liposome–DNA complexes

Vladimir P. Torchilin*†, Tatyana S. Levchenko*, Ram Rammohan*, Natalia Volodina*, Brigitte Papahadjopoulos-Sternberg‡, and Gerard G. M. D'Souza*

*Department of Pharmaceutical Sciences, Northeastern University, 360 Huntington Avenue, Boston, MA 02115; and ‡Nano Analytical Laboratory, 3951 Sacramento Street, San Francisco, CA 94118

Liposomes modified with TAT peptide (TATp-liposomes) showed fast and efficient translocation into the cell cytoplasm with subsequent migration into the perinuclear zone. TATp-liposomes containing a small quantity ($\leq$10 mol %) of a cationic lipid formed firm noncovalent complexes with DNA. Here, we present results demonstrating both *in vitro* and *in vivo* transfection with TATp-liposome–DNA complexes. Mouse NIH/3T3 fibroblasts and rat H9C2 cardiomyocytes were transfected with such complexes *in vitro*. The transfection with the TATp-liposome-associated pEGFP-N1 plasmid encoding for the green fluorescent protein (GFP) was high, whereas the cytotoxicity was lower than that of commonly used cationic lipid-based gene-delivery systems. Intratumoral injection of TATp-liposome–DNA complexes into the Lewis lung carcinoma tumor of mice also resulted in an expression of GFP in tumor cells. This transfection system should be useful for various protocols of cell treatment *in vitro* or *ex vivo* as well as for localized *in vivo* gene therapy.

gene delivery | green fluorescent protein | intracellular trafficking

Gene therapy is becoming an important strategy in the treatment of various diseases such as cancer (1–3), AIDS (3–5), and cystic fibrosis (6, 7). Viral vectors, the current favorites for intracellular DNA delivery, suffer from immunogenicity, nonspecificity, and inherent risks of complications such as the interference with the activity of tissue-specific promoters (8–10). Nonviral vectors such as cationic lipids/liposomes (11) are nonspecific, demonstrate low efficiency compared with viruses, and can be inactivated by pulmonary surfactants (12) and serum proteins (13). Cytotoxic reactions such as pulmonary inflammation (14), antiproliferative activity in proteoglycan-deficient cells (15), production of reactive oxygen intermediates (16), and inhibition of NO and tumor necrosis factor-α production in activated macrophages (17) were reported after cationic lipid/liposome treatments. Toxic side reactions are believed to be caused by the high content of cationic lipids (50–100 mol %) in nonviral transfection systems and are especially pronounced in proteoglycan-deficient cells (18, 19). Attempts to prepare nontoxic cationic transfection systems have been only partially successful (20, 21), and to minimize these drawbacks, *in vitro* transfection with subsequent introduction of the transfected cells or organs into recipients has been suggested. Fibroblasts transfected *in vitro* with an epidermal growth factor gene have been used successfully for wound healing (22). Experiments have also been performed with vein grafts (23), donor hearts (24), pulmonary artery segments (25), and lung transplants (26). Although in various transfection protocols a portion of the DNA is liberated into the cytoplasm (27), the endocytic route of internalization of nonviral vectors with subsequent degradation of the delivered DNA by lysosomal nucleases brings an additional problem.

An ideal vector should be efficient and nontoxic and bypass the endocytic pathway to minimize DNA degradation. Such a vector may find its application for *in vitro* transfection of cells or grafts for transplantation and for various protocols of a localized gene therapy.

In recent years, the "transduction" phenomenon was demonstrated with the transactivating transcriptional activator protein (TAT) from HIV-1 (28, 29) and other proteins (30, 31) known to enter various cells when added to the surrounding media. TAT-attached β-galactosidase was delivered in all tissues in mice, even the brain (32). Specific small regions of such proteins (10- to 16-mers), protein transduction domains (PTDs), and some other peptides also efficiently traverse biological membranes (33, 34). This process is receptor- and transporter-independent, is not endocytosis-mediated, and may target the lipid layer directly (28, 33).

The use of such peptides for drug and gene delivery across cellular membranes is getting increased attention (33). Covalent hitching of proteins, drugs, or DNA onto PTDs may allow for their transport into many cells both *in vitro* and *in vivo* (31, 32, 35, 36). TAT peptide (TATp) attached to several proteins was able to deliver them to various cells and organs in mice (31). The internalization by cells was shown to be energy-independent and nonendocytotic (37, 38). Several hypotheses have been suggested to explain this phenomenon (37, 39). However, the actual mechanism of this uptake/translocation is not clearly established yet.

Attempts have been made to use PTDs for intracellular delivery of DNA (40, 41) and even particulates (42). Although intracellular delivery of DNA can be enhanced, this approach still requires modification of DNA with PTDs. On the other hand, we have demonstrated (43) that even relatively large 200-nm liposomes can be delivered into various cells by multiple TATp molecules attached to the liposome surface (TATp-liposomes). Because nuclear localization of TAT and similar proteins and PTDs was clearly shown (37, 44), one may assume that noncovalent complexes of DNA with slightly positively charged TATp-liposomes will provide an effective transfection system. Low content of a positively charged lipid, needed in this case to complex a negatively charged DNA but not to enhance endocytosis, should make this system nontoxic. In turn, the presence of TATp may provide for a nonendocytic intracellular delivery pathway for DNA–liposome complexes and their subsequent accumulation in the nuclear compartment and enhanced recombination. Here we present results demonstrating both *in vitro* and *in vivo* transfection with nontoxic TATp-liposome–DNA complexes.

Materials and Methods

Materials. Egg phosphatidylcholine, cholesterol, phosphatidyl ethanolamine (PE), polyethylene glycol-PE (PEG-PE), dioleoyl trimethylammonium propane (DOTAP), and rhodamine-PE (Rh-PE) were purchased from Avanti Polar Lipids. *Para*-nitrophenylcarbonyl (pNP)-PEG-PE was synthesized in-house. FITC-dextran (4,400 Da), CL-4B Sepharose, and components of

buffer solutions were purchased from Sigma. Lipofectin reagent was from Invitrogen. TATp (11-mer: Tyr-Gly-Arg-Lys-Lys-Arg-Arg-Gln-Arg-Arg-Arg, 1,560 Da) was prepared by Research Genetics (Huntsville, AL)/Invitrogen. Cell culture media, RPMI medium 1640, Eagle's minimal essential medium, DMEM, serum-free medium (Complete Serum-Free), FBS, and heat-inactivated FBS, were supplied by Cellgro (Kansas City). Fluorescence-free glycerol-based mounting medium (Fluoro-mount-G) was from Southern Biotechnology Associates. A pEGFP-N1 plasmid designed for eukaryotic cell expression of the green fluorescent protein (GFP) was obtained from Elim Biopharmaceuticals (Hayward, CA).

Cell Cultures. Human breast adenocarcinoma cells (BT20) were maintained in Eagle's minimal essential medium (with 10 mM pyruvate/nonessential amino acids/L-glutamine/10% FBS). Lewis lung carcinoma (LLC) cells (established from the lung of a C57BL mouse bearing a tumor resulting from an implantation of primary LLC cells and widely used as a model for metastasis and for studying the mechanisms of cancer chemotherapeutic agents) were maintained in RPMI medium 1640 (with 10% FBS). Mouse fibroblasts (NIH/3T3, a continuous cell line of highly contact-inhibited cells that was established from NIH Swiss mouse embryo cultures in the same manner as the original random-bred 3T3 and the inbred BALB/c 3T3; the established NIH/3T3 line was subjected to more than five serial cycles of subcloning to develop a subclone with morphologic character-istics best suited for transformation assays) and rat cardiomyo-cytes (H9C2 myoblasts, a subclone of the original clonal cell line derived from embryonic BD1X rat heart tissue exhibiting many properties of skeletal muscle) were maintained in DMEM (with 10% FBS). Cell lines were from the American Type Culture Collection.

Synthesis of pNP-PEG-PE. pNP-PEG-PE was synthesized according to a procedure published by us (45). Briefly, 0.1 mmol of PE was dispersed in 8 ml of chloroform supplemented with 2 ml of triethylamine. The resulting mixture was supplemented with 0.5 mmol of PEG_{3500}-$(pNP)_2$ in 20 ml of chloroform and incubated overnight at room temperature under argon. Organic solvents were removed under vacuum. Dried lipid was dispersed in 0.01 M HCl and purified by gel filtration on CL-4B Sepharose using 0.01 M HCl as an eluent. Pooled fractions containing pNP-PEG-PE were freeze-dried, dissolved in chloroform, and stored at $-80°$C.

Preparation of TATp-Liposomes. A lipid film was prepared by rotary evaporation from a mixture of phosphatidylcholine, cholesterol, and pNP-PEG-PE (7:3:0.05 molar ratio) with traces of Rh-PE in chloroform. This film was rehydrated in a citrate buffer, pH 5.0, vortexed for 5 min, and then extruded through a polycarbonate filter (pore size, 200 nm) by using an Avanti Polar Lipids MiniExtruder. When loading with FITC-dextran was required, the latter was added as a component of the rehydration solution. The attachment of TATp to pNP groups on the liposome surface was carried out by incubating TATp with liposomes in a borate buffer, pH 8.5, overnight at room temperature. The slightly alkaline conditions allow for the coupling reaction with slow hydrolysis of unreacted pNP residues (45). Free FITC-dextran and TATp were removed by using a Bio-Gel A-1.5m column. Alternatively, presynthesized TAT-PEG-PE conjugate was added to the starting lipid mixture for liposome preparation. The size of FITC-dextran-loaded Rh-labeled TATp-liposomes was measured by dynamic light scattering on a Coulter N4 Plus submicron particle analyzer.

Preparation of TATp-Liposome–Plasmid Complexes. Liposomes for complexation with DNA did not contain any fluorescent labels but did contain up to 10 mol % of a cationic DOTAP to enhance

plasmid association. Liposomes from a mixture of phosphatidyl-choline, cholesterol, DOTAP, and pNP-PEG-PE (7:3:1:0.05 molar ratio) were prepared as described above and incubated with pEGFP-N1 overnight at 4°C. In a typical case, the lipo-some–plasmid complex containing a total of 2 mg of lipid and 200 μg of DNA was incubated with an appropriate amount of TATp overnight at pH 8.5 in a borate buffer and purified by gel filtration on a Bio-Gel A-1.5m column. The postcolumn fraction was subjected to agarose gel electrophoresis to test for the presence and intactness of the plasmid within the liposomes. To determine DNA content, the postcolumn TATp-liposome–plasmid complex-containing fraction was treated with Triton X-100 for 1 h at 37°C, to release the plasmid from the complex, and then subjected to agarose gel electrophoresis. Lipofectin–pEGFP-N1 complex was prepared according to manufacturer instructions (Invitrogen) by using same quantities and ratios of lipid and DNA (which are within the recommended limits for this preparation).

Gel Electrophoresis. Electrophoresis was performed by using the E-Gel electrophoresis system from Invitrogen/Life Technologies. A precast 0.8% E-Gel cartridge was prerun for 2 min at 60 V and 500 mA followed by loading of 1 μg of DNA samples in loading dye. Gel-running time was $\approx$50 min at 60 V and 500 mA. The gel then was photographed over a UV box (Photodyne, New Berlin, WI).

Freeze-Fracture Electron Microscopy. The sample was quenched by using the sandwich technique and liquid nitrogen-cooled pro-pane. A cooling rate of 10,000 K/sec avoids ice crystal formation and artifacts possibly caused by the cryofixation process. The fracturing process was carried out in JEOL JED-9000 freeze-etching equipment, and the exposed fracture planes were shad-owed with platinum for 30 sec at an angle of 25–35° and with carbon for 35 sec [2 kV, 60–70 mA, 1×10^{-5} torr (1 torr = 133 Pa)]. The replicas were cleaned with fuming HNO_3 for 24–36 h followed by repeated agitation with fresh chloroform/methanol [1:1 (vol/vol)] at least five times and examined with a JEOL 100 CX electron microscope.

Intracellular Trafficking of TATp-Liposomes. Intracellular trafficking and localization of TATp-liposomes were tested in BT20 cells grown on coverslips in six-well plates. At $\approx$60–70% confluency, cells were incubated with liposomes in a serum-free medium at 37°C under 6% CO_2. The medium was removed, and the cells were washed with sterile PBS, pH 7.4, after 1, 2, 4, 9, and 24 h of incubation. Coverslips were mounted cell-side down with fluorescence-free glycerol-based mounting medium and viewed by epifluorescence microscopy (Nikon Eclipse E400) and de-convolution differential interference contrast (DIC) microscopy with pseudocoloring (Axioplan 2, Zeiss).

Transfection in Vitro. NIH/3T3 or H9C2 cells grown to 60–70% confluency on coverslips were incubated in serum-free medium with TATp-liposome–plasmid complexes or liposome–plasmid complexes (in the quantity required to deliver 5 μg of DNA per 200,000 cells at a DNA concentration of 0.3 μg/μl added liposomal suspension) for 4 h at 37°C under 6% CO_2. The same quantity of Lipofectin–pEGFP-N1 complex with the same lipid-to-DNA ratio was used as the control. After incubation the medium was removed, and cells were washed twice with sterile PBS and reincubated with complete DMEM containing 10% FBS for 72 h. For flow cytom-etry (FACScan, Becton Dickinson Biosciences), NIH/3T3 cells were grown in 25-cm^2 flasks and fixed in 4% paraformaldehyde. GFP expression was visualized by light microscopy and epifluores-cence microscopy with an FITC filter.

Cytotoxicity Assay. NIH/3T3 cells were seeded in 96-well tissue-culture microtiter plates. After 24 h, the culture medium was

removed, and the cells were treated with TATp-liposomes, Lipofectin, TATp-liposome–pEGFP-N1 complex, or Lipofectin–pEGFP-N1 complex in serum-free medium. The experiments were carried out in both the absence of the plasmid at several different concentrations of low-cationic TATp-liposomes and Lipofectin and the presence of plasmid at concentrations of TATp-liposomes and Lipofectin required to provide a DNA concentration of 5 μg/ml (total lipid concentration for both preparations varied from ≈ 20 to ≈ 100 μg/ml). After 24 h, in the case of plasmid-free preparations, and 4 h, in the case of DNA-containing preparations, the medium was removed, Cell-Titer 96 Aqueous One solution (Promega) was added to each well, and the plates were reincubated for 4 h. This assay is based on the bioreduction of 4,5 dimethylthiazol-3-carboxymethoxy-phenyl-4-sulfophenyl-tetrazolium compound (Owen's reagent) into a colored soluble formazan product. The viability of cells was measured by using a plate reader (Multiscan MCC/340, Fisher Scientific) at 490 nm. Relative viability was calculated with cells treated only with medium alone as a control. The statistical treatment of the data was performed according to the Student's t test for two populations.

Transfection *in Vivo*. LLC tumors were grown in C57BL/6 mice (Charles River Breeding Laboratories) by s.c. injection of 8×10^4 LLC cells per mouse into the left flank (protocol 011022, approved by the Institutional Animal Care and Use Committee at Northeastern University on Nov. 26, 2001). Tumors were injected at four to five different spots with 100 μl of TATp-liposome–pEGFP-N1 complex in Hepes-buffered saline, pH 7.4, after they reached 5–10 mm in diameter. Mice were killed 72 h later by cervical dislocation, and excised tumors were fixed in a 4% buffered paraformaldehyde overnight at 4°C, blotted dry of excess paraformaldehyde and kept in 20% sucrose in PBS overnight at 4°C. Cryofixation was done by immersion of tissues in ice-cold isopentane for 3 min followed by freezing at −80°C. Fixed, frozen tumors were mounted in Tissue-Tek OCT 4583 compound (Sakura Finetek, Torrance, CA) and sectioned on a Leica (Deerfield, IL) Jung Frigocut 2800N. Sections were mounted on slides and analyzed by fluorescence microscopy and with hematoxylin/eosin staining. Tumor-bearing mice injected with TATp-free liposome–plasmid complexes of the same composition and noninjected mice with similar-sized tumors were used as negative controls.

Results and Discussion

Internalization and Intracellular Trafficking of TATp-Liposomes. Free FITC-dextran showed only minimal intracellular accumulation in the BT20 cells used (data not shown), whereas 200-nm Rh-labeled TATp-liposomes loaded with FITC-dextran rapidly translocated into these cells. Typical patterns of time-dependent distribution of TATp-liposomes inside individual cells are shown in Fig. 1. After 1 h, their diffuse localization within the cell cytoplasm was evident (Fig. 1*A*). Intracellular liposomes apparently remained intact within this time period, because the fluorescence of the intraliposomal (FITC-dextran) and membrane (Rh-PE) labels coincided. With time, TATp-liposomes, similar to TATp (37, 44), gradually migrate closer to nuclei, and after 2 and 4 h, a significant fraction of TATp-liposomes was seen surrounding the perinuclear region with a reduced cytoplasmic distribution (Fig. 1 *B* and *C*). At 9 h, the degradation of liposomes was observed (diffuse orange/red fluorescence in the cytoplasm and nucleus), with some liposomes remaining in the perinuclear region. However, by this time the FITC-dextran was almost totally released (diffuse green fluorescence, Fig. 1*D*). By 24 h virtually no internal or membrane label could be seen inside cells.

Our experiments clearly showed that, in good agreement with earlier observations (43), the uptake of TATp-liposomes is fast and efficient. Because of the nuclear tropism imparted by the
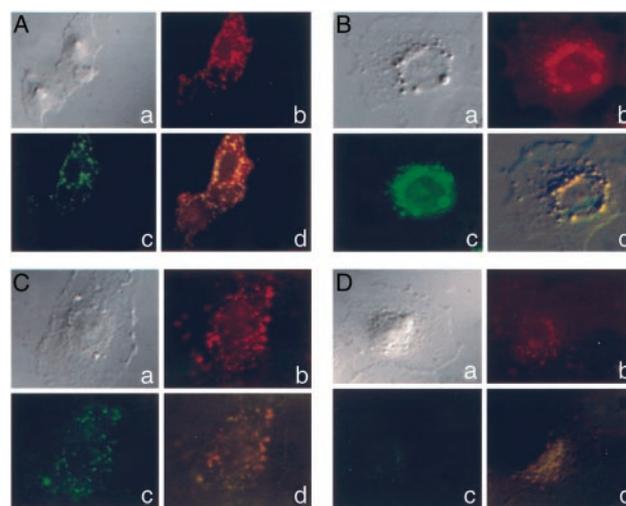

Fig. 1. Intracellular trafficking of Rh-PE-labeled and FITC-dextran-loaded TATp-liposomes within BT20 cells. Typical patterns of intracellular localization and integrity of TATp-liposome after 1 (*A*), 2 (*B*), 4 (*C*), and 9 h (*D*). *a*, DIC light; *b*, DIC with an Rh filter; *c*, DIC with an FITC filter; *d*, DIC composite of *a*–*c*. (Magnification, ×400.) For other conditions, see *Materials and Methods*.

TATp (37, 44), TATp conjugation allows for a gradual perinuclear localization of liposomes, bypassing the endocytic pathway. Eventually, liposomes are destroyed and release their contents. The relatively slow perinuclear accumulation of TATp-liposomes compared with free TATp may be explained by hindered diffusion of larger liposomal particles in the cytoplasm. However, one cannot claim the penetration of TATp-liposomes through the nuclear membrane, which was shown to form pores not larger than 26–39 nm (46). Even if TATp can allow for the pore-independent translocation of liposomes through the nuclear membrane, it has to be additionally proven in a separate experiment. From our current point of view, even if we are dealing with only an increased accumulation of DNA-bearing liposomes in the vicinity of nuclei, it still might enhance the transfection outcome. Taken together, these data support the conclusion that TATp-conjugated plasmid-bearing liposomes provide a DNA-delivery system that will bypass the lysosomal compartment and deliver its load directly into the cytoplasm and then to the vicinity of nuclei.

Preparation and Properties of TATp-Liposome–DNA Complexes. TATp-liposomes with a relatively low ($\leq$10 mol %) content of a cationic DOTAP effectively complexed and firmly retained
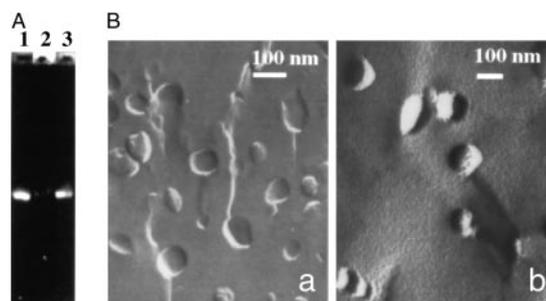

Fig. 2. (*A*) Gel-electrophoresis results of free pEGFP-N1 plasmid (lane 1), TATp-liposome–pEGFP-N1 complex (lane 2), and Triton X-100-treated TATp-liposome–pEGFP complex (lane 3). (*B*) Freeze-etching electron microscopy of TATp-liposomes (*a*) and TATp-liposome–pEGFP-N1 complex (*b*). For details, see *Materials and Methods*.
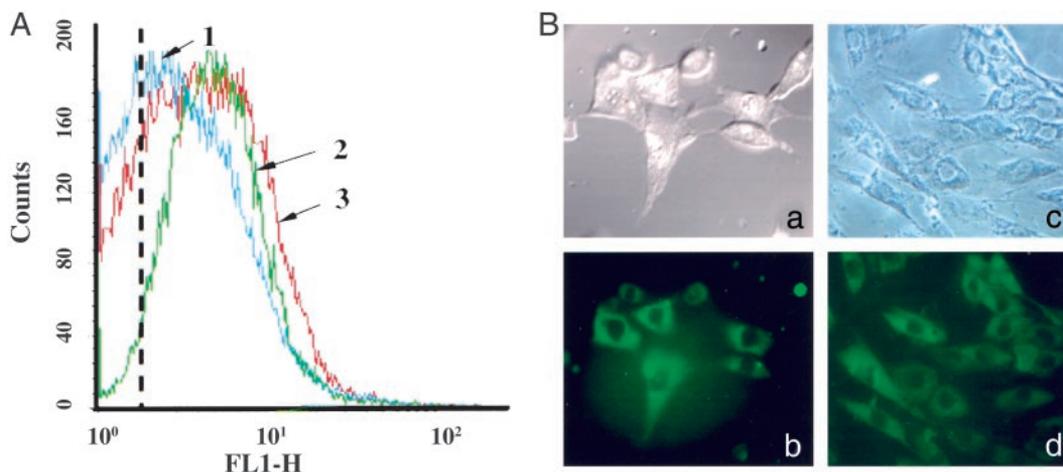
Fig. 3. Cell transfection *in vitro* with TATp-liposome–pEGFP-N1 complexes and TATp-free liposome–pEGFP-N1 complexes. (For detailed conditions, see *Materials and Methods*.) (*A*) Flow-cytometry data (the number of fluorescent cells and fluorescence intensity on the FITC channel, FL1-H, after 72 h) for NIH/3T3 cells. 1, fluorescence of cells treated with TATp-free liposome–pEGFP-N1 complex; 2, fluorescence of cells treated with an equal quantity (as DNA and lipids) of Lipofectin–pEGFP complex; 3, fluorescence of cells treated with an equal quantity (as DNA and lipids) of TATp-liposome–pEGFP complex. The dotted line shows the position of the peak autofluorescence of nontreated cells (negative control). (*B*) The microscopy (×400, after 72 h) of NIH/3T3 (*a* and *b*) and H9C2 (*c* and *d*) cells treated with TATp-liposome–pEGFP-N1 complex. (*a* and *c*) Bright-field light microscopy. (*b* and *d*) Epifluorescence microscopy with an FITC filter.

intact plasmid as evidenced by the gel-electrophoresis data (Fig. 2*A*). TATp-liposome–pEGFP-N1 complexes could not enter a gel because of their large size (Fig. 2*A*, line 2). However, after Triton X-100 treatment, all complexed DNA was released in a free form, resulting in a band with intensity close to the control-free DNA (Fig. 2*A*, compare lines 1 and 3). Depending on the type of the future experiment, the total quantity of DNA in a sample could vary from 0.05 to 0.2 μg per 1 μg of lipid, which is similar to what is normally achieved with Lipofectin (according to manufacturer instructions). Complexation of a plasmid with liposomes only moderately increased their size (from ≈150 to ≈200 nm by dynamic light scattering). The freeze-etching electron microscopy also showed that the major fraction of TATp-liposome–plasmid complexes maintained an essentially spherical shape with a size of ≈200 nm (Fig. 2*B*). Both preparations displayed convex and concave fracture planes typical of liposomal structure. The complexes were nonaggregated. Their boundaries sometimes appeared dotted, a phenomenon also observed

in other liposome–nucleic acid complexes (47). Thus, TATp-liposomes with a low content of a cationic lipid (which, in our opinion, should make the whole composition less cytotoxic) can complex and retain substantial quantities of DNA (a plasmid encoding for the formation of GFP in this particular case).

Transfection of Cells with Nontoxic TATp-Liposome–DNA Complexes *in Vitro*. The results of the treatment of NIH/3T3 fibroblasts and H9C2 cardiomyocytes with TATp-liposome–pEGFP-N1 complexes are presented in Fig. 3. The flow-cytometry data (Fig. 3*A*) show that the treatment of NIH/3T3 cells with TATp-free liposome–pEGFP-N1 complexes results in a slight increase in cell fluorescence (Fig. 3*A*, compare the position of the curve 1 peak with the dotted line showing the peak autofluorescence on nontreated cells). This fluorescence may result from some cell transfection via nonspecifically captured plasmid-bearing liposomes. At the same time, cells treated with TATp-liposome–pEGFP-N1 complexes demonstrated a substantially higher fluorescence (Fig.
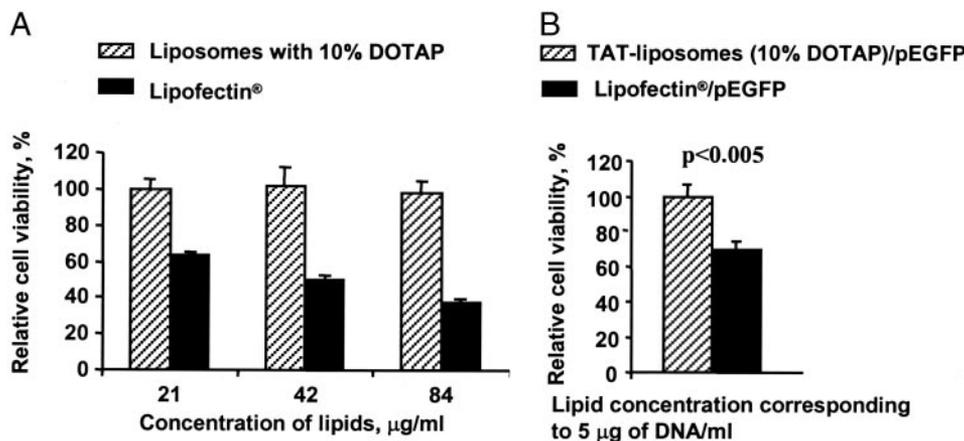

Fig. 4. Cytotoxicity test. (*A*) Comparative cytotoxicity of low-cationic TATp-liposomes and Lipofectin toward NIH/3T3 cells at different lipid concentrations. Incubation for 24 h: Cell viability in the presence of 21 μg/ml TATp-liposomes was taken as 100%. (*B*) Relative viability of NIH/3T3 cells treated with equal quantities (as DNA, at 5 μg) of TATp-liposome–pEGFP-N1 complex and Lipofectin–pEGFP-N1 lipoplex. Incubation for 4 h: Cell viability in the presence of TATp-liposome–plasmid complex was taken as 100%. For details, see *Materials and Methods*.
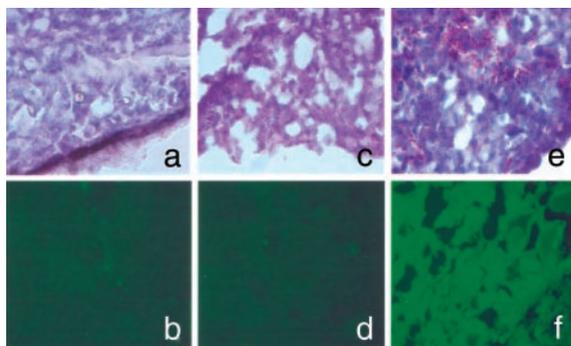
Fig. 5. *In vivo* transfection with TATp-liposome–pEGFP-N1 complex. The microscopy (×400) of frozen tissue sections from *in vivo*-growing LLC tumors in mice is shown. (*a* and *b*) Section from a nontreated tumor (background pattern). (*c* and *d*) Section from the tumor injected with TATp-free liposome–pEGFP-N1 complex. (*e* and *f*) Section from the tumor injected with TATp-liposome–pEGFP-N1 complex. (*a*, *c*, and *e*) Bright-field light microscopy after hematoxylin/eosin staining. (*b*, *d*, and *f*) Epifluorescence microscopy with FITC filter. For details, see *Materials and Methods*.

3*A*, curve 3 vs. curve 1), i.e., a higher transfection outcome. At similar conditions, Lipofectin–pEGFP-N1 complexes provided essentially the same extent of transfection and fluorescence level as TATp-liposome–plasmid complexes (Fig. 3*A*, curve 2).

Confocal microscopy confirmed the transfection of both NIH/3T3 and H9C2 cells with TATp-liposome–DNA complexes (Fig. 3*B*). From 30% to 50% of both cell types in the field of view show a bright-green fluorescence, whereas lower fluorescence was observed in virtually all cells. This outcome is similar to what was seen with Lipofectin–pEGFP-N1 complexes (25–40% of "bright" cells) and corresponds well to the published data on lipofection of, for example, dendritic cells and chondrocytes (48, 49).

An additional advantage of this system may be its lower toxicity compared with nonviral transfection systems using larger quantities of cationic lipids. We do not need to incorporate substantial quantities of cationic lipid to enhance endocytosis, because we rely here on a direct cytoplasmic delivery imparted by TATp. Small quantities of cationic DOTAP in the liposomal composition were required only to provide a firm association with negatively charged DNA. As can be seen from the photographs presented in Fig. 3*B*, the transfection was not accompanied by any visible toxic effects. All cells appear normal morphologically.

In a separate experiment, TATp-liposomes and TATp-liposome–DNA complexes were tested additionally in a direct comparative cytotoxicity assay. This assay was first performed with NIH/3T3 cells by using several different concentrations of DNA-free TATp-liposomes and Lipofectin (Fig. 4*A*). The results show that at similar concentrations, low-cationic TATp-

liposomes with 10 mol % of DOTAP were nontoxic for the cells even after 24 h of incubation, whereas the same quantities of Lipofectin caused the death of 35–65% of cells in a concentration-dependent fashion. This observation was true for the lipid concentration range between 20 and 80 μg/ml. A similar experiment performed with TATp-liposome–plasmid complex using the same quantity of Lipofectin-plasmid lipoplex as a control (5 μg of DNA and 20 μg of lipid per ml in both cases, which is a normal working concentration for the lipofection procedure), showed that the TATp-liposome–plasmid complex was ≈25% less toxic than the Lipofectin-plasmid lipoplex to the NIH/3T3 cells after 4 h of incubation (Fig. 4*B*).

Thus, complexes of DNA with TATp-liposomes, containing a small quantity of a cationic lipid (≤10 mol %) readily transfect both cancer and normal mammalian cells *in vitro* and have a relatively low cytotoxicity. It was not our goal to perform a detailed comparison of TATp-liposomes and Lipofectin in terms of their efficiency. However, we have provided good evidence that TATp-liposomes with a low content of a positively charged lipid can complex and deliver DNA into cells with less toxic effects than is typical for many nonviral DNA-delivery systems with a high content of positive charge.

Transfection of LLC Cells *in Vivo*. The final aim of this study was to attempt an *in vivo* transfection in a whole-animal model with LLC cells. We attempted a localized transfection by direct administration of TATp-liposome–pEGFP-N1 complexes into the tumor tissue to minimize the nonspecific transfection of other tissues. Fig. 5 presents the *in vivo* results with LLC cell-bearing mice. Histologically, hematoxylin/eosin-stained tumor slices in both control and experimental animals showed a typical pattern of poorly differentiated carcinoma (polymorphic cells with basophilic nuclei forming nests and sheets and containing multiple sites of neoangiogenesis; Fig. 5 *a*, *c*, and *e*). Under the fluorescence microscope, samples from control mice (nontreated mice or mice injected with TATp-free liposome–plasmid complexes; Fig. 5 *b* and *d*) showed only a background fluorescence, whereas slices from tumors injected with TATp-liposome–plasmid complexes contained bright-green fluorescence in tumor cells (Fig. 5*f*), indicating the TATp-mediated transfection *in vivo*.

Although the experiment itself is clearly of a proof-of-principle character, it is interesting to mention that the direct intratumoral administration of anticancer drugs and vaccines is getting increased attention and shows a lot of promise (50–52). Certainly, in experiments such as this one the cytotoxicity of the preparation does not represent a serious issue.

Overall, we conclude that TATp-liposome–DNA complexes should provide a useful, nontoxic means of transfection with various protocols of cell treatment *in vitro* or *ex vivo* as well as for localized *in vivo* gene therapy or DNA vaccination.

1. McCormic, F. (2001) *Nat. Rev. Cancer* **1**, 130–141.
2. Searle, P. F., Spiers, I., Simpson, J. & James, N. D. (2002) *Drug Delivery Syst. Sci.* **1**, 5–13.
3. Chang, L. J. & He, J. (2001) *Curr. Opin. Mol. Ther.* **3**, 468–475.
4. Buchschacher, G. L., Jr., & Wong-Staal, F. (2001) *Hum. Gene Ther.* **12**, 1013–1019.
5. Dornburg, R. & Pomerantz, R. J. (2000) *Adv. Pharmacol.* **49**, 229–261.
6. Suzuki, M., Matsuse, T. & Isigatsubo, Y. (2001) *Curr. Mol. Med.* **1**, 67–79.
7. Davies, J. C., Geddes, M. D. & Alton, E. W. (2001) *J. Gene Med.* **5**, 409–417.
8. Gomes-Navarro, J. & Curiel, D. T. (2000) *Lancet Oncol.* **1**, 48–58.
9. Kapturczak, M. H., Flotte, T. & Atkinson, M. A. (2001) *Curr. Mol. Med.* **2**, 245–258.
10. Buvoli, M., Langer, S. J., Bialik, S. & Leinwand, L. A. (2002) *Gene Ther.* **9**, 227–231.
11. Clark, P. R. & Hersh, E. M. (1999) *Curr. Opin. Mol. Ther.* **2**, 156–176.
12. Duncan, J. E., Whitsett, J. A. & Horowitz, A. D. (1997) *Hum. Gene Ther.* **8**, 431–438.
13. Audouy, S., Molema, G., de Leij, L. & Hoekstra, D. (2000) *J. Gene Med.* **2**, 465–476.
14. Scheule, R. K., George, J. A., Bagley, R. G., Marshal, J., Kaplan, J. M., Akita, G. Y., Wang, K. X., Lee, E. R., Harris, D. J., Jiang, C., *et al.* (1997) *Hum. Gene Ther.* **8**, 689–707.
15. Belting, M. & Petersson P. (1999) *Biochem. J.* **342**, 281–286.
16. Dokka, S., Toledo, D., Shi, X., Castranova, V. & Rojanasakul, Y. (2000) *Pharm. Res.* **17**, 521–525.
17. Filion, M. C. & Phililips, N. C. (1997) *Biochim. Bhiophys. Acta* **1329**, 345–356.
18. Plank, C., Mechtler, K., Szoka, F. C., Jr., & Wagner, E. (1996) *Hum. Gene Ther.* **7**, 1437–1446.
19. Belting, M. & Petersson, P. (1999) *J. Biol. Chem.* **274**, 19375–19382.
20. Floch, V., Loisel, S., Guenin, E., Herve, A. C., Clement, J. C., Yaouanc, J. J., des Abbayes, H. & Ferec, C. (2000) *J. Med. Chem.* **36**, 4617–4628.
21. Choi, J. S., Lee, E. J., Jang, H. S. & Park, J. S. (2001) *Bioconjugate Chem.* **12**, 108–113.

22. Rosenthal, F. M., Cao, L., Tanczos, E., Kopp, J., Andree, C., Stark, G. B., Mertelsmann, R. & Kulmburg, P. (1997) *In Vivo* **11,** 201–208.
23. Bai, H. Z., Bai, H. Z., Sawa, Y., Zhang, W. D., Yamakawa, T., Morishita, R., Kaneda, Y. & Matsuda, H. (1998) *Ann. Thorac. Surg.* **66,** 814–819.
24. Dalesandro, J., Akimoto, H., Gorman, C. M., McDonald, T. O., Thomas, R., Liggitt, H. D. & Allen, M. D. (1996) *J. Thorac. Cardiovasc. Surg.* **111,** 416–421.
25. Yano, M., Hiratsuka, M., Mora, B. N., Scheule, R. K. & Patterson, G. A. (1999) *Ann. Thorac. Surg.* **68,** 1810–1814.
26. Boasquevisque, C. H., Mora, B. N., Boglione, M., Ritter, J. K., Scheule, R. K., Yew, N., Debruyne, L., Qin, L., Bromberg, J. S. & Patterson, G. A. (1999) *J. Thorac. Cardiovasc. Surg.* **117,** 8–14.
27. Zelphati, O. & Szoka, F. C., Jr. (1988) *Proc. Natl. Acad. Sci. USA* **93,** 11493–11498.
28. Frankel, A. D. & Pabo, C. O. (1988) *Cell* **55,** 1189–1193.
29. Vocero-Akbani, A., Lissy, N. A. & Dowdy, S. F. (2000) *Methods Enzymol.* **322,** 508–521.
30. Joliot, A., Pernelle, C., Deagostini-Bazin, H. & Prochiantz, A. (1991) *Proc. Natl. Acad. Sci. USA* **88,** 1864–1868.
31. Fawell, S., Seery, J., Daikh, Y., Moore, C., Chen, L. L., Pepinsky, B. & Barsoum, J. (1994) *Proc. Natl. Acad. Sci. USA* **91,** 664–668.
32. Schwarze, S. R., Ho, A., Vocero-Akbani, A. & Dowdy, S. F. (1999) *Science* **285,** 1569–1572.
33. Plank, C., Zauner, W. & Wagner, E. (1998) *Adv. Drug Delivery Rev.* **34,** 21–35.
34. Schwartz, J. J. & Zhang, S. (2000) *Curr. Opin. Mol. Ther.* **2,** 162–167.
35. Gius, D. R., Ezhevsky, S. A., Becker-Hapak, M., Nagahara, H., Wei, M. C. & Dowdy, S. F. (1999) *Cancer Res.* **59,** 2577–2580.
36. Lee, H. J. & Pardridge, W. M. (2001) *Bioconjugate Chem.* **12,** 995–999.
37. Vives, E., Brodin, P. & Lebleu, B. (1997) *J. Biol. Chem.* **272,** 16010–16017.
38. Derossi, D., Joliot, A. H., Chassaing, G. & Prochiantz, A. (1996) *J. Biol. Chem.* **271,** 18188–18193.
39. Prochiantz, A. (1999) *Ann. N.Y. Acad. Sci.* **886,** 172–179.
40. Eguchi, A., Akuta, T., Okuyama, H., Senda, T., Yokoi, H., Inokuchi, H., Fujita, S., Hayakawa, T., Takeda, K., Hasegawa, M. & Nakanishi, M. (2001) *J. Biol. Chem.* **276,** 26204–26210.
41. Snyder, E. L. & Dowdy, S. F. (2001) *Curr. Opin. Mol. Ther.* **3,** 147–152.
42. Lewin, M., Carlesso, N., Tung, C.-H., Tang, X.-W., Cory, D., Scadden, D. T. & Weissleder, R. (2000) *Nat. Biotechnol.* **18,** 410–414.
43. Torchilin, V. P., Rammohan, R., Weissig, V. & Levchenko, T. (2001) *Proc. Natl. Acad. Sci. USA* **98,** 8786–8791.
44. Truant, R. & Cullen, B. R. (1999) *Mol. Cell. Biol.* **19,** 1210–1217.
45. Torchilin, V. P., Levchenko, T. S., Lukyanov, A. N., Khaw, B. A., Klibanov, A. L., Rammohan, R., Samokhin, G. P. & Whiteman, K. R. (2001) *Biochim. Biophys. Acta* **1511,** 397–411.
46. Pante, N. & Kann, M. (2002) *Mol. Biol. Cell* **13,** 425–434.
47. Jääskeläinen, I., Sternberg, B. J. Mönkkönen, J. & Urtti, A. (1998) *Int. J. Pharm.* **167,** 191–203.
48. Pecher, G., Spahn, G., Schirrmann, T., Kulbe, H., Ziegner, M., Schenk, J. A. & Sandig, V. (2001) *Anticancer Res.* **21,** 2591–2596.
49. Stove, J., Fiedler, J., Huch, K., Gunther, K. P., Puhl, W. & Brenner, R. (2002) *Osteoarthritis Cartilage* **10,** 212–217.
50. Goldberg, E. B., Hadba, A. R., Almond, B. A. & Marotta, J. S. (2002) *J. Pharm. Pharmacol.* **54,** 159–180.
51. Haroun, R. I. & Brem, H. (2000) *Curr. Opin. Oncol.* **12,** 187–193.
52. Amiji, M. M., Lai, P. K., Shenoy, D. B., Rao, M. (2002) *Pharm. Dev. Technol.* **7,** 195–200.

MEDICAL SCIENCES